

$\Lambda \rightarrow N\pi$ process with an external diagram and the quark mass shift

S. Y. Yoo and Il-Tong Cheon

Department of Physics, Yonsei University, Seoul, 120-749, Korea

(Received 11 June 1999; published 30 December 1999)

The $\Lambda \rightarrow N\pi$ process is calculated in a bag model by including an external diagram. The energy shift of quarks in the propagator is considered and the weak process is described with a four point effective Lagrangian. As a result, a right relative sign between the parity conserving and parity nonconserving amplitudes is obtained. The branching ratio $\Gamma_{\Lambda \rightarrow p\pi^-} / \Gamma_{\Lambda \rightarrow N\pi}$ is also shown to agree well with experimental data.

PACS number(s): 13.30.Eg, 13.75.Ev

I. INTRODUCTION

In the analysis of a nonleptonic decay amplitude, traditionally, the method of calculating the parity violating (PV) amplitude is different from that of the parity conserving (PC) part. The former, which corresponds to a pion s wave, is obtained by current commutation, while the latter, corresponding to a pion p wave, is calculated by the baryon pole approximation. Since the 1980s, this nonleptonic decay process has been studied in terms of the quark by many authors [1–3]. Although they could not fully explain the experimental results of all nonleptonic hyperon decay processes, it is believed that these approaches are not absolutely wrong.

In this work, we follow the formalism given in Ref. [2]. The main characteristic of Ref. [2] is that the s - and p -wave amplitudes are obtained in a consistent procedure such as the low energy strong interaction between quarks in baryons and mesons described by chiral symmetry and confinement, and the weak interaction is introduced, imposing local gauge invariance of the whole strong Lagrangian under $SU(2)_L \otimes U(1)$ transformations. In this sense it seems to be more elegant than other approaches. But the result in Ref. [2] is not reasonable because it gives the wrong relative sign to the s and p terms in comparison with the experimental data.

In order to explain the experimental data more reasonably, we modify this formalism in the following three ways. First, we calculate an external contribution which is not considered in Ref. [2]. This term, called “separable,” was considered in terms of an $SU(3)$ parameter in Ref. [1]. Retaining self-consistency, we derive it in a natural manner from the same formalism as that given in Ref. [2]. Moreover, it is shown to yield a very meaningful contribution to the parity conserving amplitude. Second, we describe this nonleptonic process with the effective Lagrangian constructed by a one gluon exchange correction [4–6]. This Lagrangian makes the $\Delta I = 3/2$ contribution sufficiently small in our case. Finally, when the internal transition in the p -wave part occurs, the

intermediate state can be described as a baryon pole. We thus reexamine this pole structure by the quark mass in the propagator by the amount of baryon mass difference in initial (final) and intermediate states.

II. THEORY

The Lagrangian describing the nonleptonic weak process, which is evaluated with one gluon exchange and renormalization group scaling [4,6,7], is

$$\mathcal{L} = \frac{1}{2\sqrt{2}} G \sin \theta_C \cos \theta_C (a_3 \mathcal{L}_3 + a_6 \mathcal{L}_6), \quad (1)$$

where θ_C is the Cabibbo angle and $\mathcal{L}_{3,6}$ are given as

$$\mathcal{L}_{3,6} = (\bar{u}^i \gamma_L^\mu s_i)(\bar{d}^j \gamma_{\mu L} u_j) \mp (\bar{u}^i \gamma_L^\mu u_i)(\bar{d}^j \gamma_{\mu L} s_j), \quad (2)$$

with $\gamma_L^\mu = \gamma^\mu (1 - \gamma_5)$. In Eq. (2), the negative (positive) sign refers to \mathcal{L}_3 (\mathcal{L}_6). The subscripts 3 and 6 indicate the dimensions of the $SU(3)$ color group of the final state $\mathbf{3} \otimes \mathbf{3} = \mathbf{6} \oplus \bar{\mathbf{3}}$, and i, j represent the color indices. $a_3 \approx 2.1$ and $a_6 \approx 0.4$ which are evaluated at $\mu \approx 1$ GeV and $\alpha_s(\mu) \approx 0.4$ with one gluon exchange or $a_3 \approx 1.5$ and $a_6 \approx 0.8$ [8] with renormalization group scaling. Group structure tells us that \mathcal{L}_3 allows a $\Delta I = 1/2$ transition while \mathcal{L}_6 includes both $\Delta I = 1/2$ and $3/2$.

For the $\Lambda \rightarrow p\pi^-$ process, we have to consider the quark diagrams shown in Fig. 1. Among those diagrams, (a)–(c) are called internal graphs and (d) is an external graph. The internal graphs contribute only to the \mathcal{L}_3 transition channel, because minus signs (originating from color, anticommuting of fermions, and Fierz rearrangement) appear when the initial quark legs s, u in $(\bar{u}s)(\bar{d}u)$ are exchanged. However, in the case of the external diagram, the hadronic matrix element is $\langle p | \bar{u}s | \Lambda \rangle \langle \pi^- | \bar{d}u | 0 \rangle$ and the factor $+1/3$ appears due to the color degree of freedom when the initial quark legs are

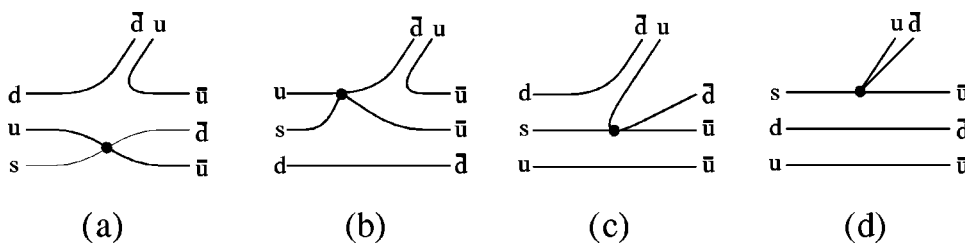


FIG. 1. These graphs are possible processes we considered here for the $\Lambda \rightarrow p\pi^-$ decay: (a), (b), and (c) represent internal processes and (d) is the external process.

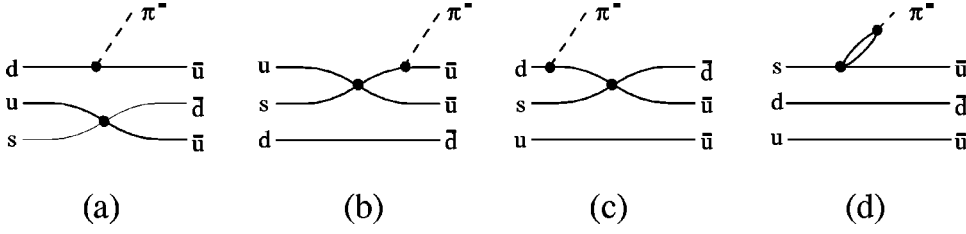


FIG. 2. Diagrams generated by the time ordering in the brackets of Eq. (4). Each diagram represents two cases $x_0 > y_0$ and $y_0 > x_0$, where x and y are the interaction points of $\bar{d}u\pi^-$ and $(\bar{u}s) \times (\bar{d}u)$, respectively.

exchanged. Thereby, the first and second terms of Eq. (2) do not cancel each other and accordingly this external diagram contributes to both \mathcal{L}_3 and \mathcal{L}_6 channels. Thus the $\Lambda \rightarrow N\pi$ matrix element can be written as

$$\begin{aligned} \langle p\pi^- | \Lambda \rangle &= -a_3(A_i - A_e) + 2a_6A_e, \\ \sqrt{2}\langle n\pi^0 | \Lambda \rangle &= a_3(A_i - A_e) + 2a_6A_e, \end{aligned} \quad (3)$$

where A_e and A_i stand for contributions from external and internal graphs of $(\bar{u}s)(\bar{d}u)$ in the $\Lambda \rightarrow n\pi^0$ process. Needless to say, the small portion of $\Delta I = 3/2$ comes from the A_e in Eq. (3).

To evaluate the internal and external contributions to the $\Lambda \rightarrow N\pi$ process in a consistent way, we make use of the formalism of Ref. [2]. In this scheme the $B' \rightarrow B\pi$ amplitude is expressed as

$$\begin{aligned} A_{B'B\pi} &= \langle B, \pi_{out} | B'_{in} \rangle \\ &= \int dx^4 dy^4 \phi_\pi^*(x) \langle B_{out} | T \mathcal{L}(y) J_{\pi_i}(x) \delta_S | B'_{out} \rangle, \end{aligned} \quad (4)$$

where J_π is a pion source term,

$$J_{\pi_i}^i(x) = (i/2f_\pi) \bar{q}(x) \gamma_5 \tau^i q(x), \quad (5)$$

$\phi_\pi(x)$ is the pion wave function in spherical cavity mode, and δ_s is the surface delta function.

The diagrams to be considered are presented in (a)–(d) of Fig. 2 which correspond to each graph in Fig. 1. Hence diagram (d) is the newly considered process in this paper which is named the external diagram.

With the usual bag solution in Ref. [9] and the detailed calculation method given in Refs. [2] and [10], we can write the matrix element as

$$A_{\Lambda \rightarrow p\pi^-} = 2\pi \delta(E_\pi + E_p - E_\Lambda) \chi_p^\dagger (S - P \boldsymbol{\sigma} \cdot \hat{\mathbf{k}}) \chi_\Lambda, \quad (6)$$

where S and P denote parity violating and conserving parts expressed as

$$\begin{aligned} S(P) &= \frac{G}{2f_\pi} \sin \theta_C \cos \theta_C [a_3 \{S_i(P_i) + S_e(P_e)\} \\ &\quad + 2a_6 S_e(P_e)]. \end{aligned} \quad (7)$$

The subscripts in $S(P)_{i,e}$ denote the internal and external contributions. The internal parts are calculated in the form

$$\begin{aligned} S_i &= \frac{R^2 \varphi_0(kR)}{4\pi\sqrt{6}} \sum_n \{T_s(\omega'_n) + T_s(-\omega_n)\}, \\ P_i &= \frac{R^2 \varphi_1(kR)}{4\pi\sqrt{6}} \sum_n \{T_p(\omega_n) + T_p(-\omega'_n)\}, \end{aligned} \quad (8)$$

where $\varphi_l(kR)$ is the radial part of the pion wave function with angular momentum l and R is the bag radius. While the first term in the summation of Eq. (8) is a result of the process including the quark propagator, the second one results from the process including the antiquark propagator. ω_n is the n th term of the series of eigenvalues satisfying bag boundary condition $j_0(\omega_n R) = j_1(\omega_n R)$ and ω'_n is $j_0(\omega'_n R) = -j_1(\omega'_n R)$.

In Eq. (8), $T_s(\omega_n)$ and $T_p(\omega_n)$ are given as

$$\begin{aligned} T_s(\omega_n) &= 4\{(\omega_0, \omega_0)(\omega_n, p_s) - (\omega_0, \omega_n)(\omega_0, p_s)\} / \\ &\quad D(\omega_0, -\omega_n) - 6(\omega_0, \omega_0)(\omega_n, p_s) / D(-\omega_0, \omega_n), \\ T_p(\omega_n) &= \left\{ \frac{8}{3}(\omega_0, \omega_0)(\omega_n, p_s) + \frac{4}{3}(\omega_0, \omega_n) \right. \\ &\quad \left. \times (\omega_0, p_s) \right\} / D(\omega_0, -\omega_n) - 6(\omega_0, \omega_0) \\ &\quad \times (\omega_n, p_s) / D(-\omega_0, \omega_n), \end{aligned} \quad (9)$$

where the term which contains $D(\omega_0, -\omega_n)$ in the denominator comes from diagram (b) and the term which has $D(-\omega_0, \omega_n)$ is from (c) in Fig. 2. Here the following notation is used:

$$\begin{aligned} (\alpha, \beta)(\gamma, p_s) &= N_\alpha N_\beta N_\gamma N_s \int_0^R dr r^2 [j_0(\alpha r) j_0(\beta r) \\ &\quad + j_1(\alpha r) j_1(\beta r)] [j_0(\gamma r) j_0(p_s r) \\ &\quad + \Omega_s j_1(\gamma r) j_1(p_s r)], \end{aligned} \quad (10)$$

and

$$\frac{1}{D(\alpha, \beta)} = N_\alpha N_\beta \frac{2j_0(\alpha R) j_0(\beta R)}{E_\pi + \alpha + \beta}. \quad (11)$$

N_α is a normalizing constant of the bag solution with energy ω_α and j_l is the spherical Bessel function. The p_s , m_s , and ω_s stand for the momentum, mass, and energy of s quark, respectively, and Ω_α is $p_\alpha / (\omega_\alpha + m_\alpha)$. The external parts calculated in the same way are given as

$$S_e = \frac{6R^2\varphi_0(kR)}{4\pi\sqrt{6}} \sum_{m,n} \{L_s(\omega_m, \omega_n) - L_s(\omega'_m, \omega'_n) - L_s(-\omega_m, -\omega_n) + L_s(-\omega'_m, -\omega'_n)\}$$

$$P_e = \frac{4R^2\varphi_1(kR)}{4\pi\sqrt{6}} \sum_{n,m} \{-L_p(\omega_m, \omega'_n) + L_p(-\omega_m, -\omega'_n)\}, \quad (12)$$

where

$$L_s(\omega_n, \omega_m) = \{(\omega_0, \omega_m)(\omega_n, -p_s) + (\omega_0, \omega_n)(\omega_m, -p_s) - (\omega_m, \omega_n)(\omega_0, -p_s)\} / D(-\omega_m, -\omega_n),$$

$$L_p(\omega_m, \omega'_n) = \{(\omega_0, \omega_m)(\omega'_n - p_s) + (\omega_0, \omega'_n)(\omega_m, -p_s) + (\omega_m, \omega'_n)(\omega_0, -p_s)\} / D(-\omega_m, -\omega'_n). \quad (13)$$

On the other hand, diagram (a) in Fig. 2, which gives only the p wave, can be calculated as

$$P'_i = \frac{N_0^6 R^2 j_0(\omega_0 R)^2}{\sqrt{6} E_\pi} 6(\omega_0, \omega_0)(\omega_0, p_s) \leftarrow (x_0 < y_0) - \frac{N_0^6 R^2 j_0(\omega_0 R)^2}{\sqrt{6} E_\pi} 6(\omega_0, \omega_0)(\omega_0, p_s) \leftarrow (y_0 < x_0), \quad (14)$$

and consequently, this term vanishes as was seen in Ref. [2].

In this stage, we have to make some comment on the above results. The numerical estimate of S and P does not reproduce well the experimental data. This situation was seen in Ref. [2] also. The difference between our result and that of [2] is whether diagram (d) of Fig. 2 is taken into account in the effective Lagrangian. But these effects cannot be so large as to alter the sign of the p part changes because they relate to the $\Delta I = 3/2$ transition which should be small in the context of the $\Delta I = 1/2$ rule. Accordingly, the baryon pole contribution must be taken into account.

To describe the pole structure consistently, we do not alter the above equation except to introduce an effective mass m^* to the quarks in the propagator. It means that, when process (b) in Fig. 2 is considered, the series of eigenvalues is shifted by linking up with the boundary condition $j_0(p_n R) = \Omega_n j_1(p_n R)$ and the shifted ground state energy $\omega_0^* = \sqrt{p_0^2 + m^{*2}}$ satisfies

$$\omega_0^* - \omega_0 \approx M_\Sigma - M_\Lambda, \quad (15)$$

which is the difference between initial (Λ) and intermediate (Σ) state energies. This alters the second term of $T_p(\omega_n)$ as

$$-6(\omega_0, \omega_0)(p_n, p_s) / D(-\omega_0, \omega_n^*), \quad (16)$$

with $j_1(p_n r) \rightarrow \Omega_n j_1(p_n r)$ and $N_n \rightarrow N_{\omega_n^*, p_n, m^*}$.

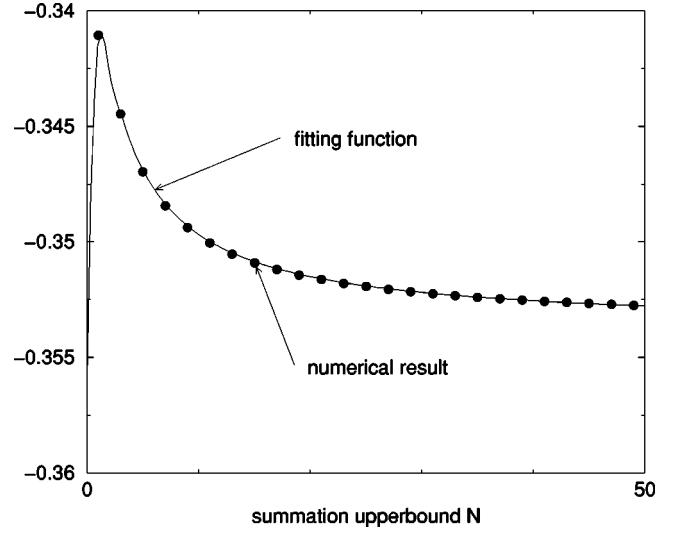


FIG. 3. The points represent numerical results of S_e at $R=0.5$ fm as a function of the summation upper bound N and the solid line represents the fitting function of those points, which is $-(4.26 + 15.7/N + 19.8 \tan^{-1}N) \times 10^{-2}$.

The first term of $T_p(\omega_n)$ is not affected by this procedure because intermediate (n) and final (p) states have almost the same static energy. Note that the $T_p(-\omega'_n)$ term in Eq. (9) is not affected by the mass shift, because this contains anti-quark propagation and, therefore, it does not form the baryon pole. Since P'_i in Eq. (14) has no quark propagator, it has nothing to do with the effective quark mass shift and, then, it also vanishes.

In a numerical estimate, it is enough to consider the first few terms of the summation in evaluating the internal amplitudes, because it converges very rapidly. However, in the case of external amplitudes, the double summation makes a very slow convergence and we have to carry out the summation over a somewhat large number of terms. This tendency can be seen in Fig. 3. If the quark in the effective Lagrangian is a massless free Dirac field, the external amplitudes vanish because of the γ algebra. Hence we strongly believe that the appearance of this quantity comes from the quark confinement.

In addition, we can analyze the behavior of the external amplitudes at $\omega_n, \omega_m \gg 1$. For a brief case, let $m_s \approx 0$ and $\omega_n, \omega_m \gg E_\pi$; then the L_s can be written as

$$L_s \approx \sum_{n,m} \frac{\omega_n \omega_m}{(\omega_n + \omega_m)^2} \int_0^R dr r^2 [j_0^2(\omega_0 r) + j_1^2(\omega_0 r)] \times [j_0(\omega_m r) j_0(\omega_n r) - j_1(\omega_m r) j_1(\omega_n r)] \approx \text{const} \times \sum_{m,n} \frac{\omega_m R + \omega_n R + 2\omega_m \omega_n R^2}{\omega_m \omega_n (\omega_m + \omega_n)^3 R^5}. \quad (17)$$

Obviously, this summation is convergent. Note that the external diagram is not always convergent. When considering the penguin type of one gluon exchange diagram, we are faced with the $O_{5,6} \approx (\bar{d}s)_L (uu + \bar{d}d)_R$ operators. If one does

TABLE I. The ratio of the decay width, $\Gamma_{\Lambda \rightarrow p \pi^-} / \Gamma_{\Lambda \rightarrow n \pi^-}$.

R	0.4	0.5	0.6	0.7	0.8	0.9	Expt. in Ref. [11]
$a_3 \approx 2.1, a_6 \approx 0.4$	0.644	0.640	0.637	0.636	0.638	0.644	0.641
$a_3 \approx 1.5, a_6 \approx 0.8$	0.653	0.651	0.650	0.650	0.652	0.655	0.641

the same calculation in Eq. (17) with those operators, it gives a logarithmic divergence. This is reasonable since the external amplitudes of $O_{5,6}$ are divergent when a massless free quark is engaged.

Even though the external diagram is divergent mathematically, it is no serious problem in this case. When the energy ω_n reaches the M_W region, the effective Lagrangian reveals the W boson propagator and therefore we can deduce that it moderates the logarithmic divergence. As a result, it is enough to sum over the energy eigenvalues at $\omega_n \approx M_W$ when we evaluate the external amplitudes.

III. RESULTS AND DISCUSSION

Because the dependence of the m_s is very weak, we fixed the mass of the s quark as 200 MeV in our calculations. One can see almost the same result as that obtained with the mass fixed to zero.

Table I shows the ratio of the decay rate $\Gamma_{\Lambda \rightarrow p \pi^-} / \Gamma_{\Lambda \rightarrow n \pi^-}$ versus R . The experimental value is well reproduced around $R \approx 0.6$ fm with $a_3 \approx 2.1$ and $a_6 \approx 0.4$ and, accordingly, the $\Delta I = 3/2$ channel is sufficiently suppressed at that range of R . There are two reasons for the suppression of the $\Delta I = 3/2$ channel. One of them is the one gluon exchange effect, i.e., $a_3/a_6 \approx 5$, and the other is the relatively small contribution of the external part, i.e., $S_e/S_i \approx 0.04$ at $R \approx 0.7$ fm.

On the other hand, with $a_3 \approx 1.5$ and $a_6 \approx 0.8$, we can see that the ratio $a_3/a_6 \approx 2$ is insufficient to suppress the $\Delta I = 3/2$ channel and, accordingly, the theoretical values are relatively worse than before.

Table II shows S and P versus R together with the experimental values. In this table, we can see that experimental values of S and P are well reproduced at $R = 0.6 - 0.7$ fm, and they have the right relative signs.

At this stage, it is worth comparing our result of the p part with that of Ref. [3]. The authors of Ref. [3] described the intermediate state with a static baryon wave function to give the baryon pole for the case of the p part, while the s part was estimated with a quark propagator.

To see the difference between these two methods explicitly, let a_3 and a_6 be unity and exclude the external contribution and only consider the leading term ($n=0$) of the

TABLE II. s and p of $\Lambda \rightarrow p \pi^-$ decay with $a_3 \approx 2.1$ and $a_6 \approx 0.4$.

R	0.60	0.65	0.70	0.75	Exp.
s	4.20	3.17	2.43	1.90	3.25×10^{-7}
p	1.24	1.11	1.00	0.90	1.18×10^{-7}

internal contribution with no mass shift in the form factor. Then the P_i in Eq. (8) can be written as P_{i0} :

$$P_{i0} = -6F/(M_\Sigma - M_N) + 4F/(M_\Lambda - M_N), \quad (18)$$

where

$$F = \frac{N_0^6 R^2 j_0(\omega_0 R)^2}{\sqrt{6}} (\omega_0, \omega_0)(\omega_0, p_s). \quad (19)$$

If P'_i in Eq. (14), which vanishes in our scheme, has a baryon pole structure, we can write it in the form

$$P'_i = -6F/(M_\Sigma - M_N) + 6F/(M_\Lambda - M_N). \quad (20)$$

One can see that $P'_i + P_{i0}$ is none other than the Λ_-^0 of the p part in Ref. [3]. As a result, we find that the Λ_-^0 of the p part in Ref. [3] represents the leading term of the radial excitation in our result. From the above analysis, one can see the difference feature between the results of our scheme and those of Ref. [3]. While the amplitude of (a) in Fig. 2 vanishes in our case, it gives an important contribution in Ref. [3]. Accordingly, we can see that the external contribution is important in the case of the P part as shown in Table III.

Though it is impossible to separate P'_i and P_{i0} in the scheme of Ref. [3] alone, this is possible by comparing P_{i0} and P'_i with Ref. [3]; that is to say, we can simply deduce that the first term of P'_i corresponds to Fig. 2(a) with $x_0 < y_0$ and the first term of P_{i0} to Fig. 2(c). This relation can be seen more explicitly by considering the $\Lambda \rightarrow n \pi^0$ process rather than the $\Lambda \rightarrow p \pi^-$ process. The amplitude of the $\Lambda \rightarrow n \pi^0$ process with $x_0 < y_0$ in Ref. [3] can be written as

$$\langle n | \bar{u} s \bar{d} u | \Sigma^0 \rangle \langle \Sigma^0 | \bar{u} u - \bar{d} d | \Lambda \rangle, \quad (21)$$

and $\langle n | \bar{u} s \bar{d} u | \Sigma^0 \rangle \langle \Sigma^0 | \bar{u} u | \Lambda \rangle$ is obviously possible only through a Fig. 2(c) type diagram, while $\langle n | \bar{u} s \bar{d} u | \Sigma^0 \rangle \langle \Sigma^0 | -\bar{d} d | \Lambda \rangle$ is possible only through a Fig. 2(a) type diagram. In a detailed calculation, the results of the

TABLE III. P amplitude for $R = 0.6 - 0.9$.

R	0.6	0.7	0.8	0.9×10^{-7}
P in [3]	0.774	0.484	0.320	0.221×10^{-7}
P_i	0.20	0.181	0.158	0.135×10^{-7}
P_e	0.238	0.177	0.136	0.108×10^{-7}

two cases are identical as the $\Lambda \rightarrow p\pi^-$ process does. In addition, we can easily see the same correlation in the $y_0 < x_0$ case between the $\Lambda \rightarrow p\pi^-$ and $\Lambda \rightarrow n\pi^0$ processes, and accordingly, the $\Delta I = 1/2$ rule is satisfied with each of the internal diagrams of Fig. 2 separately in our case and in Ref. [3], respectively.

ACKNOWLEDGMENTS

This work was supported by the Korean Science and Engineering Foundation (Grants Nos. 976-0200-002-2 and 961-0204-018-2) and the Korean Ministry of Education (Grants Nos. 98-015-D00061 and 1998-001-D00249).

-
- [1] J.F. Donoghue and E. Golowich, Phys. Rev. D **14**, 1386 (1976); H. Galic, D. Tadic, and J. Trampetic, Nucl. Phys. **B158**, 306 (1979); J. F. Donoghue *et al.*, Phys. Rev. D **21**, 186 (1980); D. Tadic and J. Trampetic, *ibid.* **23**, 144 (1981).
- [2] P. Gonzalez, S. Noguera, J. Bemabeu, and V. Vento, Nucl. Phys. **A423**, 477 (1984).
- [3] J.A. Oteo and S. Noguera, Phys. Lett. **161B**, 377 (1985).
- [4] M.K. Gaillard and B.W. Lee, Phys. Rev. Lett. **33**, 108 (1974).
- [5] M.A. Shifman, A.I. Vainshtein, and V.J. Zakharov, Nucl. Phys. **B120**, 315 (1977).
- [6] C.G. Callan, R.F. Dashen, and D.J. Gross, Phys. Rev. D **19**, 1826 (1979).
- [7] L.B. Okun, *Leptons and Quarks* (North-Holland, New York, 1982).
- [8] J.F. Donoghue, E. Golowich, and B.R. Holstein, *Dynamics of the Standard Model* (Cambridge University Press, Cambridge, England, 1992).
- [9] G.A. Miller, A.W. Tomas, and S. Theberge, Phys. Lett. **91B**, 1912 (1980).
- [10] O.V. Maxwell and V. Vento, Nucl. Phys. **A407**, 366 (1983).
- [11] Particle Data Group, C. Caso *et al.*, Eur. Phys. J. C **3**, 9 (1998).